Crystal growth inhibition by mobile randomly distributed stoppers

James P. Lee-Thorp,[*,†] Alexander G. Shtukenberg,[*,‡] and Robert V. Kohn[*,†]

†*Courant Institute of Mathematical Sciences, New York University, NY, USA*

‡*Department of Chemistry, New York University, NY, USA*

E-mail: leethorp@cims.nyu.edu; shtukenberg@mail.ru; kohn@cims.nyu.edu

Abstract

Crystal growth is inhibited by the presence of impurities. Cabrera and Vermilyea introduced a model in 1958, in which the impurities are modelled as immobile stoppers. The quantitative consequences of this model have mainly been explored for the special case where the stoppers are immobile and arranged in a periodic array. Here we use numerical simulation to explore what happens when the stopper locations are randomly distributed and the stoppers have finite lifetimes. As this problem has just two nondimensional parameters, namely nondimensionalized versions of the mean stopper distance and the mean stopper lifetime, we are able to explore a large region of the parameter space using simulation.

The stopper density is measured by the percolation parameter, a nondimensionalized inverse distance between stoppers, ζ. Our results show that when the stopper density is relatively small (ζ below about 0.8), the macroscopic velocity of the step is roughly the same for randomly-located stoppers as for a periodic array of stoppers. Moreover, in this regime the average velocity is almost independent of the stopper lifetime. For large stopper densities (more precisely, when the percolation parameter

ζ is above about 0.8) the situation is entirely different. For periodically-placed immobile stoppers, the average velocity drops sharply to 0 at $\zeta = 1$. For randomly-located immobile stoppers, by contrast, the average velocity remains positive for ζ well above 1, and it approaches 0 gradually rather than abruptly. For randomly-located stoppers with finite lifetimes, the average velocity has a nonzero asymptote for large ζ; thus, for large stopper densities, the average velocity depends mainly on the mean stopper lifetime. In this regime the inhibition kinetics predicted by our model resemble those of the Bliznakov kink blocking mechanism.

Introduction

Additives and impurities play a major role in controlling crystal growth kinetics. Understanding the mechanisms responsible for crystal-additive interaction is one of the primary tasks of crystal growth science and is important for numerous applications. The most profound growth inhibition occurs when impurities and additives adsorb to the crystal surface, becoming stoppers that interfere with propagation of the growth step over the surface.[1–3] This mechanism was modeled in 1958 by Cabrera and Vermilyea, who considered step propagation in the presence of strongly adsorbed stoppers.[4] The step cannot go through stoppers, but it can advance in the regions between them. Doing so increases the curvature κ of the moving front; due to the Gibbs-Thomson effect this leads to a higher step free energy and slower step advancement. If the stopper separation is large enough, the parts of the step on the two sides of the stopper eventually merge; this permits the step to proceed, leaving the stopper behind. If the stopper separation is small enough, however, the step reaches a stationary state and its progress is arrested.

To make the model quantitative, Cabrera and Vermilyea considered the case when the stopper locations form a periodic array of size d. When d is smaller than the diameter of the critical nucleus, $2r_c$, the step reaches a stationary state and growth is arrested, leading to the so-called "dead zone." On the other hand, if the percolation parameter $\zeta = 2r_c/d < 1$,

the step's progress is slowed but not arrested by the stoppers. If we approximate the part of the step between two stoppers as a piece of a circle, we see that the step breaks past a row of stoppers at the moment when its curvature is $\kappa = 2/d$; this is the time when the velocity of the step reaches its minimum $V_{\min} = V_0(1-\zeta) > 0$. The step breaks past the stoppers because neighboring segments collide, forming a continuous step which quickly becomes nearly flat. The step then proceeds at velocity V_0 until it encounters the next row of stoppers. Cabrera and Vermilyea provided an approximate expression for the average step velocity V_{avg} in this context:

$$V_{\text{avg}} = V_0\sqrt{1-\zeta}. \tag{1}$$

The C-V formula (1) provides a good qualitative description of the growth inhibition process, including the formation of a dead zone. However, it does not agree quantitatively with experimental data.[5–20]

This discrepancy is not surprising since the C-V formula was developed using numerous assumptions. Indeed, the model of Cabrera and Vermilyea implicitly assumes that: (1) Steps have high kink density; (2) Steps are characterized by isotropic edge energies and kinetic coefficients; (3) Crystallization occurs close to equilibrium; (4) Stoppers are large, i.e. cannot be overgrown by the step fluctuations; and (5) Contact with the stopper does not reduce the step's free energy leading it to wrap quickly around and overgrow the stopper. The model also assumes that (6) Stoppers adsorb immediately and never desorb; and the C-V formula (1) was derived assuming that (7) Stoppers are distributed on the crystal surface in a square grid. Much work has been done to address the discrepancy between modeling and experiment by modifying some of these hypotheses. Improved agreement has, for example, been achieved by using a different expression for the driving force of crystallization,[8,9] by playing with adsorption isotherms[8,9,21] or by considering a slow rate of adsorption.[10,12,18,22–26] In addition, in some cases researchers have developed models combining several inhibition mechanisms,[8,9] played with mathematical expressions for the average growth rate,[8,9,27] or considered formation of macrosteps.[28,29] Potapenko obtained an approximation better than

eqn (1), for the average velocity in the original C-V setting with a periodic array of stoppers.[30] While this work has achieved important insight in specific cases, overall it has not overcome the shortcomings associated with the assumptions (1) – (7) of the C-V model, and it has not achieved a satisfactory description of experimental data.

A convenient way to avoid some of the preceding assumptions is to use kinetic Monte-Carlo simulations. This approach has been used, for example, to study steps on the {001} surface of a Kossel crystal for random and regular distributions of stoppers,[31–34] different stopper sizes,[31,32] different bond energies/kink densities,[31,35–37] stoppers varying in their ability to be overgrown[35] and in their mobility,[32] and surfaces developing macrosteps.[38,39] Ice crystallization in the presence of antifreeze proteins has also been simulated using molecular dynamics.[40] Such simulations can capture many qualitative features of growth kinetics, but they are not well-suited for making quantitative comparisons to experiments, since they rely on specific models of the surface and there are many parameters associated with the intermolecular interactions.

Recently we implemented a semi-implicit front-tracking scheme to develop the picture of Cabrera and Vermilyea and show that moderate step anisotropy does not change the average growth rate significantly.[41] Here we use the same approach and return to the original C-V model, relaxing just the last two assumptions (numbers 6 and 7) listed above. Specifically: we use the same continuum model as Cabrera and Vermilyea, but *our stopper locations are random*, and we consider the possibility that *stoppers desorb at random times*. Our starting point is the observation that this model involves just two nondimensional parameters: a "percolation parameter" ζ (which can be viewed as the nondimensionalized typical inverse distance between stoppers), and a second parameter μ (a nondimensionalized measure of the stopper lifetime); as a result, it is feasible to explore the entire parameter space using numerical simulation. (For the definitions of ζ and μ see eqns (3) and (9) respectively.) Our simulations use periodic boundary conditions (so the growth takes place in a strip $0 < x < L$) and front-tracking (solving a nonlinear PDE for the evolving position of the front). Since the

problem is stochastic, for each choice of the parameters we do many runs and average the results. In addition to kinetic Monte-Carlo simulations,[31,32] the Cabrera-Vermilyea model with randomly-located immobile stoppers was previously simulated by Miura, using a phase field method;[42] however our simulations are better-resolved and more numerous, and we are therefore able to extract more information from them.

Our results show that when the percolation parameter ζ is less than about 0.8 the average velocity of the step is roughly the same for randomly-located stoppers as in the periodic case, and it is almost independent of the stopper lifetime. In this regime, the numerically-determined average velocity is somewhat larger than that predicted by the C-V expression (1) and somewhat smaller than that predicted by Potapenko's formula[30].

For larger ζ the situation is very different. For periodically-placed immobile stoppers, the average velocity drops sharply to 0 at $\zeta = 1$. For randomly-located immobile stoppers, by contrast, the average velocity remains positive for ζ well above 1, and it approaches 0 gradually rather than abruptly. Our method does not permit identification of a critical value ζ_c where the average velocity becomes 0, however, our results are consistent with the estimate by Potapenko[43] that $\zeta_c \approx 1.33$. For randomly-located stoppers with *finite* lifetimes, the average velocity has a nonzero asymptote for large ζ; thus, when $\zeta \gg 1$ the average velocity depends mainly on the mean stopper lifetime. In this regime the inhibition kinetics predicted by our model resemble those of the Bliznakov kink blocking mechanism.

Modeling

Our recent work[41] simulated the motion of step past a periodic array of stoppers. Here the situation is quite different, because the stopper locations are *random*. Since the problem is intrinsically stochastic, the evolving step is a random interface, whose properties must be explored by sampling. Moreover, in the random setting, distant parts of the step can collide with one another, something that does not happen in the periodic setting. Thus,

the presence of random stoppers introduces numerical challenges beyond those considered in our prior work. However, the basic physics – the step motion law – is the same as in our previous paper. On the other hand, one way in which our current setting is simpler, is that our previous paper considered the effect of a highly-anisotropic surface energy, whereas in this work we consider only the isotropic case. We believe, however, based on our previous publication[41], that our results should also be applicable for anisotropic surface energy if the anisotropy is not very great.

Step motion law

The normal velocity of a curved step can be expressed as:

$$V = V_0(1 - \omega\gamma\kappa/\Delta\mu) = M\sigma\left(1 - \frac{\xi}{\sigma}\kappa\right). \tag{2}$$

Here, $V_0 = M\sigma$ is the velocity of a straight step, κ is the step's curvature, $\Delta\mu$ is the difference in chemical potentials between the crystal and the growth medium, γ is the surface energy, ω is the molar volume, M is the mobility or kinetic coefficient, σ is the dimensionless supersaturation, and ξ is a dimensional parameter related to the radius r_c of the critical nucleus by $\xi/\sigma = r_c$. This law applies away from the stoppers; the velocity is, of course, 0 at a stopper. As a result, the evolving step consists, in general, of many separate curves, each ending at a stopper. These curves evolve independently by the motion law (2), until

(i) the two curves on opposite sites of a stopper become (nearly) tangent;

(ii) some curve encounters a new stopper; or

(iii) two curves collide.

When (i) occurs the two curves merge, leaving the stopper behind. When (ii) occurs, the curve that encountered the stopper gets broken into two curves. When (iii) occurs there is a topological transition.

Our steps are nearly always "pinned," in the sense that they include some stoppers. If ξ is large enough compared to the typical distance between stoppers, the step will reach a stationary state, i.e. it will get "stuck," at least until some stopper disappears. For a periodic array of stoppers this is familiar: if distance between stoppers is d then the critical value of ξ at which the step becomes stationary is $\xi_c = d\sigma/2$. Notice that in the random setting as well as in the periodic one, a stationary step consists of pieces of circles, each of radius ξ/σ. If the step is not stationary, then at least one of its component curves has nonzero velocity (the evolving piece of the step will typically not have constant curvature).

Similar considerations apply as σ varies, with ξ held fixed: if σ is small enough then the interface will get stuck. When the stoppers form a periodic array, the critical value of σ (when the interface gets stuck) is $\sigma_c = 2\xi/d$. Note that $\xi/\xi_c = \sigma_c/\sigma = 2\xi/(\sigma d)$.

For randomly-placed stoppers, we do not have a simple criterion for the threshold at which the surface gets stuck. Nevertheless, it is convenient to nondimensionalize ξ. Therefore, we introduce the *percolation parameter* ζ:

$$\zeta = \frac{\xi}{\xi_c} = \frac{2\sqrt{\lambda}}{\sigma}\xi, \tag{3}$$

where λ is the stopper density and $\xi_c = \sigma/(2\sqrt{\lambda})$. It is convenient to set

$$d = \frac{1}{\sqrt{\lambda}}, \quad \text{so that} \quad \xi_c = \frac{d\sigma}{2}; \tag{4}$$

these definitions are consistent with those introduced above in the periodic setting. We note, however, that in the random setting the step does not necessarily get stuck when $\zeta > 1$ (so ξ_c is not a critical value above which the step gets stuck); moreover, in the random setting the mean distance between stoppers is not exactly d but a multiple of d. (For the 2D Poisson point process with density λ, the mean distance from a point to its nearest neighbor is $1/(2\sqrt{\lambda})$; in view of eqn (4) this is $d/2$.)

Our problem is well-suited to numerical study since the motion law (2) involves just

one nondimensional parameter, namely ζ. While our simulations were naturally done using nondimensionalized variables, our results will be reported in terms of dimensional parameters such as V, ξ, and σ.

Stoppers

A simulation must be done in a finite domain. Ours were done in a strip: $0 < x < 1$, with periodic boundary conditions in x. Thus, our stoppers are randomly located in the strip, but our simulation assumes the presence of "image stoppers" periodically located with respect to x. The use of periodic boundary conditions inevitably introduces finite-size effects; we shall discuss some of them below. One expects and our simulations will confirm that the finite-size effects are insignificant when the typical distance between stoppers is much smaller than the width of the strip and the percolation parameter is well below the critical percolation value, ζ_c, where the front gets stuck.

A simulation must be initialized. We took our initial interface to be straight, at the bottom of the strip. The initial condition is, in practice, quickly forgotten.

The only stoppers that matter are those that the interface might soon encounter. Therefore we start the simulation by choosing the locations of the stoppers in the rectangle $0 < x < 1$, $0 < y < 1/10$. To simulate randomly-located stoppers with density λ, we choose the number of stoppers in the box by drawing from a Poisson distribution with mean $\lambda/10$, then we choose the location of each stopper by independent trials from a uniform distribution on $[0, 1] \times [0, 0.1]$. When the maximum height of the interface approaches $y = 1/10$, we use the same protocol to determine the number and placement of stoppers in the next region $[0, 1] \times [0.1, 0.2]$, and so on. Since we do our numerics in nondimensional variables,

$$\lambda_0 = \text{the expected number of stoppers in a } 1 \times 1 \text{ box} \tag{5}$$

is a key numerical parameter. Taking it large helps avoid finite-size effects, but makes the

simulation less efficient. We tried values up to $\lambda_0 = 40$; however most of the simulations reported in what follows used $\lambda_0 = 20$.

In some of our simulations the stoppers are immobile, i.e. they never disappear. In others they are "mobile," i.e. they disappear randomly, so they have finite lifetimes. This is modeled by assigning to each stopper a nondimensional lifetime, chosen from an exponential distribution with a fixed mean τ_s. In dimensional variables, this corresponds to typical stopper lifetime

$$\tau_{sc} = \tau_s \frac{L}{M\sigma} \tag{6}$$

where L is the width of the strip, and M and σ are, respectively, the mobility coefficient and dimensionless supersaturation introduced earlier. Evidently, τ_s is the ratio of the dimensional lifetime τ_{sc} to the time $L/(M\sigma)$ it would take a flat interface moving at velocity $V_0 = M\sigma$ to traverse an $L \times L$ computational box in the absence of stoppers. We note that if the stoppers are mobile, then the actual stopper density is not constant; rather, at the time t_k when the region $k/10 < y < (k+1)/10$ first gets its stoppers the density there is λ_0, but as the stoppers disappear the density decreases with time:

$$\lambda(t) = \lambda_0 e^{-(t-t_k)/\tau_s} \tag{7}$$

We shall explain below how we processed our data to correct for this phenomenon.

As noted earlier, the evolving front consists, at any time, of a collection of curves (whose endpoints are at stoppers). As the curves on opposite sides of a stopper progress, the angle between them, the "pinning angle" ϕ (Figure 1), will typically decrease. When it reaches a critical value ϕ_c (the "pinning angle breakthrough threshold") the two curves merge and advance unimpeded, leaving the stopper behind. The choice of ϕ_c is a modeling decision; it is natural to use a small positive value, to capture the effect of microscopic fluctuations, which we do not explicitly represent. For the simulations presented here, we used the value $\phi_c = 5.8°$, which was used in our previous publication.[41]

Figure 1 provides a schematic of the evolving front. We are mainly interested in its average vertical velocity. In calculating the average velocity of a single run we naturally discard the initial transient, using only data from the second half of the simulated time interval ($10 < t < 20$). For a single run, the average velocity over a given time period is computed using the step's average height at the beginning and end of the period. Since the problem is stochastic we use ensemble averaging as well as time averaging; for a given set of parameter values, we typically did 50 runs and averaged the results.

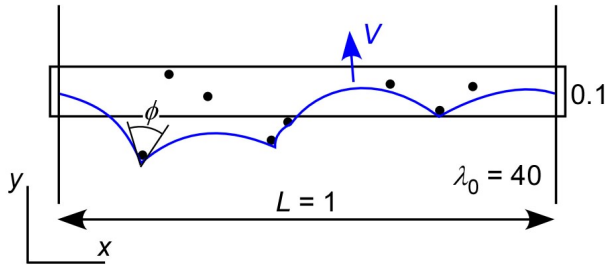

Figure 1: Schematic description of our numerical scheme: the stoppers are randomly located in a strip of width $L = 1$. The only stoppers that matter are those near the front; in the simulation, we populate 1×0.1 rectangles with stoppers one at a time, each rectangle being populated when it becomes relevant. The periodic boundary condition in x assures that the step's macroscopic direction of motion is vertical. The step breaks past a stopper when the pinning angle ϕ at that stopper reaches the breakthrough threshold ϕ_c.

A typical example of a run using immobile stoppers, done with $\zeta = 0.5$, is available in the Supporting Information (Video S1).

Numerical methods

At any given time the front consists of a collection of curves, pinned at their endpoints by stoppers, moving with normal velocity equal to a constant times $(1 - C\kappa)$, with C being a positive constant. The simulation of this motion law is by now rather routine. We use the same semi-implicit scheme as in our prior work,[41] specialized to the isotropic setting of the present paper (for a detailed account of this scheme, see the Supporting Information of that paper). The use of a semi-implicit scheme is convenient, since it permits us to use relatively large time steps. To maintain spatial accuracy, the discretization of each curve is equispaced

with respect to arc length. This is maintained by redistributing the grid points at each time step.

The list of curves (and endpoints) changes at selected times, when (i) the pinning angle breakthrough threshold is reached at a particular stopper, (ii) the evolving front encounters a new stopper, (iii) the front collides with itself, or (iv) a stopper that's on the front disappears. At such times the data structure changes: a new list of curves (and endpoints) is identified and discretized, then the evolution continues. The simulation must, of course, be vigilant in watching for these events. In particular, it must monitor the pinning angles, the distance to the nearest stopper, and the distance between the curves that make up the front.

Some mathematical issues

This paper explores how the macroscopic velocity of the step depends on the density and evaporation rates of the stoppers. Our operational definition of the macroscopic velocity is simply $\Delta y/\Delta t$, where Δy is the change in the average height of the step over a long time interval and Δt is the length of that time interval.

We are assuming that the macroscopic velocity is a well-defined random variable, so that its mean value can estimated by averaging many samples. While this assumption seems reasonable, we are not aware of a mathematically rigorous justification. The existence of a macroscopic velocity *has* been proved[44] for an interface moving with normal velocity $V = f(x) - \kappa$, where f is a random function of position satisfying certain conditions. One could mimic our problem by taking f to be zero on small randomly-placed balls (the stoppers) and a nonzero constant elsewhere. Unfortunately, such an f is not permitted by the existing theory, since for a 1D curve moving in the plane the theory requires f to be Lipschitz continuous with $f - |\nabla f|$ everywhere positive. (There is reason to think a similar result might hold for more general f; indeed, when f is periodic in space rather than random and the focus is on a 1D curve moving in the plane, the macroscopic velocity exists[45] under substantially milder conditions on f.)

A small-slope approximation to the motion law $V = f(x) - \kappa$ is obtained by taking the step to be the graph of a function $u(x,t)$ satisfying $u_t = u_{xx} + f(x, u(x,t))$; here $f(x,u)$ is again a random function of two variables. In this setting there is somewhat more theory, with far fewer requirements on f (for example it can be negative). In many applications it is natural to vary the driving force while holding the heterogeneity fixed; this is modeled by considering the equation $u_t = u_{xx} + f(x, u(x,t)) + F$ where F is constant. When the heterogeneity is strong enough one expects there to be critical values $F_1 \leq F_2$ such that the interface gets stuck for $F < F_1$ and it has positive average velocity for $F > F_2$. Rigorous results of this type have been known for some time in the spatially-periodic setting[46] (where $F_1 = F_2$), and they have been extended to the random setting.[47,48] A key question is whether $F_1 = F_2$, in other words: *if the interface doesn't get stuck, is its average velocity necessarily positive*? It is easy to imagine that the answer might be negative in a regime where interface gets locally stuck, making progress only due to "rare events" (for example, in the context of stoppers, the existence of regions in which the stoppers are anomalously sparse). An interface that moves but has macroscopic velocity 0 is said to be "sub-ballistic." Sub-ballistic interface motion has been ruled out in some settings but shown to occur in others.[49,50]

It is an open question whether sub-ballistic motion can occur in our setting (with immobile stoppers). Indeed, our percolation parameter plays a role analogous to that of the driving force F in the preceding discussion. When ζ is large enough we expect the interface to get stuck; when ζ is small enough we expect it to have positive average velocity. We wonder whether there might be an interval of ζ's for which the interface doesn't get stuck but its average velocity is 0.

Results and discussion

Immobile stoppers

For a periodic array of stoppers, the step gets stuck at the first row of stoppers if $\zeta \geq 1$, and its motion is time-periodic if $\zeta < 1$ (after an initial transient). In the present setting – immobile stoppers randomly located in a strip, simulated with periodic boundary conditions in x – the situation is very different: the evolving step is sure to get stuck eventually. Indeed, the number and arrangement of stoppers near height y is a random variable (independent of y); a configuration dense enough to entirely stop the step is a rare event if ζ is small, but if one waits long enough (i.e. considers a large enough interval in y) such a configuration will eventually occur.

This is a finite-size effect: a step encountering random stoppers in all space ($-\infty < x < \infty$) would not get stuck due to an unusually dense collection of stoppers in a finite region; rather, it would break through at larger or smaller x where the configuration is more typical. Real crystals are finite too, but this finite-size effect is much more significant in our numerical setting than in the real world. When ζ is small the configurations that arrest the step are very rare, so the step is unlikely to get stuck within the timeframe of our simulation. Once ζ gets close to 1, however, a significant fraction of the simulations get stuck within the computational timeframe. This occurs for two reasons: as ζ increases (i) the configurations capable of stopping the step become less rare; and (ii) the correlation length ℓ (between different parts of the step) increases, since the step is more likely to have parts that are locally stuck. (We expect the importance of finite-size effects to be governed by ℓ/L, where L is the width of the computational strip.)

Figure 2 shows the distribution of final average step heights, across 50 runs done at different values of $\zeta = \xi/\xi_c$. (These simulations were done, as usual, in a strip of width 1 with periodic boundary conditions, and each run was stopped at $T = 20$. For these tests, the mean number of stoppers in a 1×1 box was taken to be $\lambda_0 = 40$.) When $\zeta = 0$ the

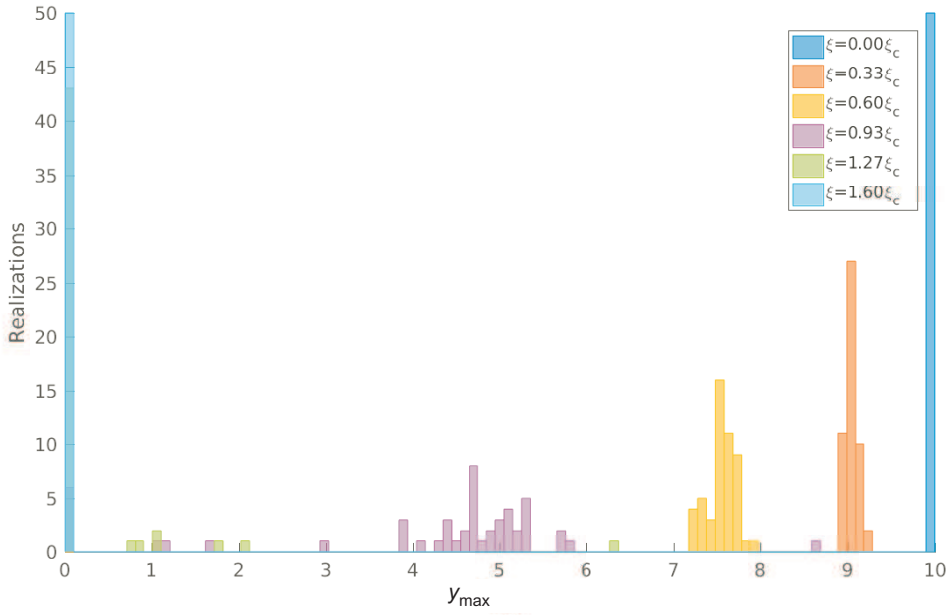

Figure 2: Distribution of the final average heights ($y_{\max}$). These simulations were done in a strip of width 1 with periodic boundary conditions, stopping at $T = 20$. The mean number of stoppers in a 1×1 box was $\lambda_0 = 40$. For each value of $\zeta = \xi/\xi_c$ the distribution reflects the outcome of 50 simulations.

stoppers have no effect and every run has the same final position V_0T. For $\zeta = 0.33$ and $\zeta = 0.60$ few if any runs get stuck; however the distribution of average velocities gets wider as ζ increases. At $\zeta = 0.93$ the distribution is extremely broad, and the finite-size effect discussed above is evident. At $\zeta = 1.27$ most of the runs got stuck very early, though a few never got stuck and one reached an average height larger than $0.6V_0T$. At $\zeta = 1.60$ almost all the runs got stuck, and those that didn't still made such limited progress that their final average step height was less than $0.01V_0T$.

Our main goal, for immobile stoppers, is to estimate the dependence of V_{avg}/V_0 on ζ for a strip of infinite width, where finite-size effects are not present. Therefore – to avoid contamination by finite-size effects – we *excluded* the runs that got stuck from our calculation of the average velocity.

The green, red, yellow, and blue curves in Figure 3(a) show the average velocity of the evolving front as a function of the percolation parameter ζ. The colors correspond to different

choices for the mean number of stoppers λ_0 in our 1×1 computational box (recall, from our discussion of the modelling, that this parameter controls the magnitude of the finite-size effects). For ζ below about 0.5 the curves associated with different choices of λ_0 coalesce – an indication that finite-size effects are unimportant in that regime. At $\zeta \approx 0.5$ the curve associated with $\lambda_0 = 5$ begins to lag (*i.e.* the associated value of $V_{\rm avg}$ is smaller than those obtained using $\lambda_0 = 10$, 20, and 40). At a larger value of ζ the curve associated with $\lambda_0 = 10$ begins to lag, and at a still larger value (around $\zeta = 0.7$) the curve associated with $\lambda_0 = 20$ begins to lag relative to the one associated with $\lambda_0 = 40$. These results suggest that for ζ greater than about 0.8, finite-size effects lead our method to slightly underestimate $V_{\rm avg}$, even for the runs using $\lambda_0 = 40$.

While finite-size effects are surely present for large ζ, our simulations in that regime are still interesting. For each of our choices of λ_0, the average velocity became very small around $\zeta = 1.25$, although the average velocity remained positive (in particular, at least one of our 50 runs did not get completely stuck within the computational timeframe) even at $\zeta = 1.6$. These results seem quite consistent with the estimate by Potapenko[43] that for the motion of a step in the presence of immobile random stoppers, the threshold where $V_{\rm avg}/V_0$ becomes zero is about $\zeta = 1.33$.

It is interesting to compare the results just discussed to what happens for periodically-placed stoppers. The curve marked by black diamonds in Figure 3(a) shows the actual average velocity, determined numerically.[41] For ζ below about 0.8 the qualitative behavior of $V_{\rm avg}/V_0$ is very similar in the periodic and random settings, though the value is slightly smaller when the stoppers are random. For ζ well above 0.8 the two models are very different, since $V_{\rm avg}/V_0$ approaches 0 sharply at $\zeta = 1$ for periodic stoppers, whereas in the random setting the graph has a flat tail, approaching 0 only as ζ increases past about 1.25.

We have thus far discussed only numerical results. In the periodic setting there are two well-known "approximate formulas" for $V_{\rm avg}/V_0$: The C-V eqn (1)[4] and a formula obtained by Potapenko.[30] The solid black and magenta curves in Figure 3(a) show the output of

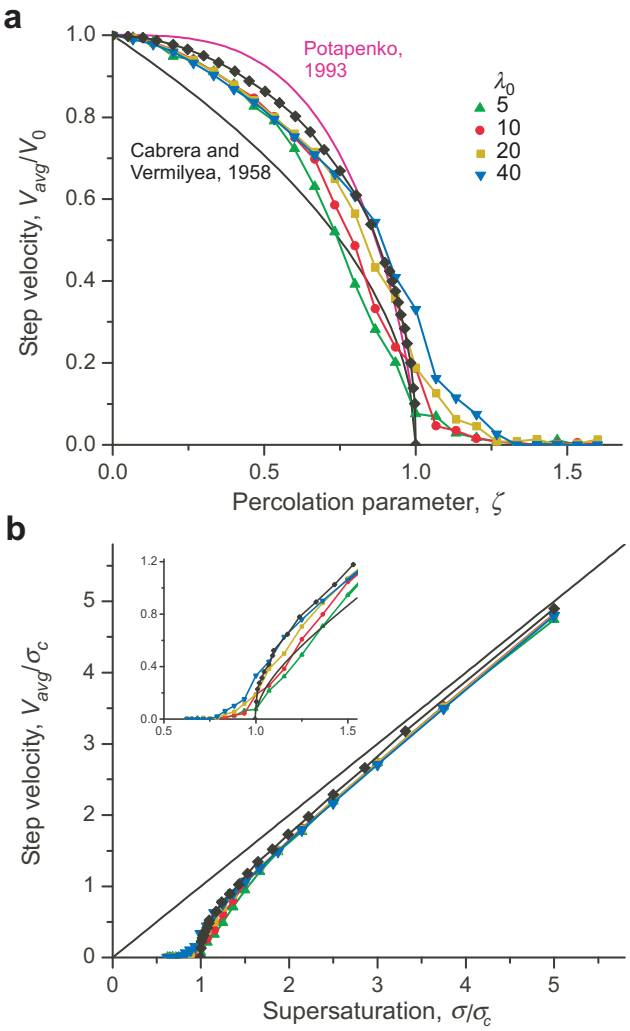

Figure 3: Average step velocity as a function of **(a)** the percolation parameter $\zeta = \xi/\xi_c$ and **(b)** the supersaturation σ/σ_c, for random immobile stoppers. The green, yellow, red, and blue curves show results obtained using different choices of λ_0 (the number of stoppers in the simulation box λ_0). For comparison, results are also shown for the case when the stoppers form a periodic array (black diamonds; these are exact results, obtained numerically). The black and magenta solid curves in plot (a) are the predictions of two approximate formulas developed with the periodic case in mind: the original proposal of Cabrera and Vermilyea (our eqn (1)) and one due to Potapenko.[30] The inset in plot (b) gives a magnified view of the region where the average velocity transitions from 0 to positive, as the supersaturation σ increases.

these formulas. Their qualitative behavior is similar to the simulations; however, when ζ is relatively small the C-V formula (1) substantially underestimates the average velocity and Potapenko's formula substantially overestimates it.

Figure 3(b) provides a different view of the same data: it shows how the average velocity depends on the supersaturation σ. We use there the convention that

$$\sigma_c = 2\xi\sqrt{\lambda} = \frac{2\xi}{d},$$

so that $\sigma/\sigma_c = 1/\zeta$ and a step gets stuck in the periodic setting precisely when $\sigma < \sigma_c$. The figure plots V_{avg}/σ_c against $\sigma/\sigma_c = 1/\zeta$. The asymptotically linear behavior seen for large σ/σ_c is no surprise: for small values of ζ we have $V_{\text{avg}} \approx V_0 = M\sigma$, so $V_{\text{avg}}/\sigma_c \approx M(\sigma/\sigma_c)$. The vanishing of the velocity for small σ/σ_c is also no surprise, since the step gets stuck when ζ is large enough. The key difference between the C-V and random models lies in *how* the average velocity approaches 0. The inset in Figure 3(b) captures this difference by providing a magnified view of the relevant part of the graph.

We have focused thus far on the step's average velocity, but its roughness is also of interest. Figure 4 reports the observed average roughness as a function of $\zeta = \xi/\xi_c$. In this figure, what we report as roughness is the average (over samples that didn't get stuck) of the rms height, computed as $\left(\frac{1}{N}\sum_{i=1}^{N}(y_i - \overline{y})^2\right)^{1/2}$, where $\{y_i\}$ are the heights of an equispaced (with respect to arclength) discretization of the front and $\overline{y}$ is the average height. As in Figure 3, we provide data using several different choices for the mean number of stoppers λ_0 in our 1×1 computational box. For values of ζ up to about 0.8 the roughness increases almost linearly with ζ, and the results are essentially independent of λ_0. For larger values of ζ the results show a lot of scatter; note that a significant fraction of the steps get stuck within the computational timeframe in this regime, so the roughness is estimated by averaging a relatively small ensemble. The approximately linear dependence of roughness on ζ can be understood as follows: once ζ is large enough to significantly slow the front, we expect from

the growth law $V = V_0(1 - \xi\kappa/\sigma)$ that the local curvature of the front will be of order σ/ξ. Dimensional analysis suggests that the roughness should behave like 1/curvature. Since $\zeta = \xi/\xi_c = 2\xi/(d\sigma)$, this suggests a roughness of order $\xi/\sigma = (d/2)\zeta$.

Since step velocity decreases as ζ increases, step roughness should increase as V/V_0 decreases. This effect has been observed experimentally for various systems, and has been discussed quantitatively for *L*-cystine growing by the motion of steps in the presence of the growth inhibitor *L*-cystine dimethylester.[19]

Stoppers with finite lifetimes

In real systems, stoppers are rarely completely immobile. Indeed, stoppers may disappear due to desorption from the surface; or they may suddenly become irrelevant, if fluctuations permit the step to overgrow a stopper even when the pinning angle (the angle ϕ in Figure 1) is larger than the breakthrough threshold. These two mechanisms are indistinguishable macroscopically if the growth conditions are constant. They can, however, be distinguished by varying the supersaturation, since the desorption rate is independent of supersaturation, while the statistics of growth step fluctuations should depend on supersaturation. In this paper we focus on desorption, i.e. on stoppers that disappear from the surface. Our stoppers disappear randomly (each stopper's lifetime is an independent, exponentially-distributed random variable). The stopper disappears at the end of its lifetime, whether or not it is pinning the evolving step. Since we are modeling desorption, our stoppers' lifetimes are independent of supersaturation; however our data could, with appropriate processing, be used to make predictions for stoppers whose disappearance rates have a known dependence on supersaturation.

When each stopper has a finite lifetime the average velocity of the step must be positive. Indeed, if ζ is large then the step might get stuck transiently; but it is sure to make further progress when the stoppers that pin it eventually disappear. Doing simulations with mobile stoppers is only marginally more difficult than with immobile ones: one must simply remem-

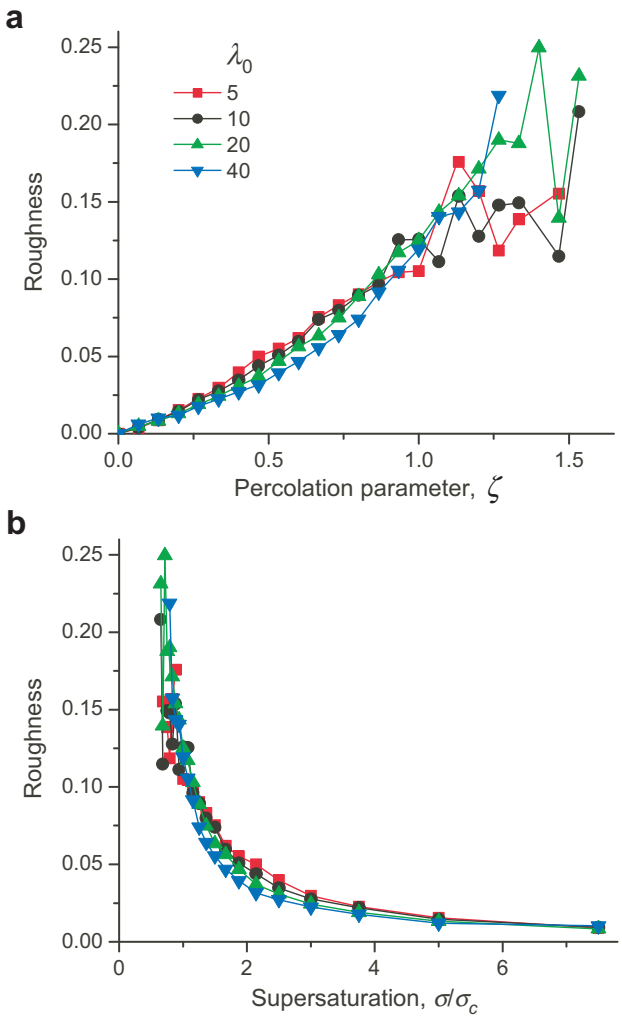

Figure 4: Step roughness as a function of the percolation parameter $\zeta = \xi/\xi_c$ **(a)** and supersaturation $\sigma/\sigma_{c,0}$ **(b)** for random immobile stoppers. The results are presented for different choices of λ_0 (the expected number of stoppers in a 1×1 box within our computational strip $0 < x < 1$).

ber to remove the stoppers when their lifetimes expire. However the interpretation of the output has subtleties that weren't present in the immobile case, as we'll explain presently.

Figure 5 is the finite-stopper-lifetime analogue of Figure 3: it shows the average velocity of the step for several different values of the expected nondimensional stopper lifetime τ_s (defined in terms of the dimensional lifetime τ_{sc} by eqn (6)). In this figure, which presents our computational results with a minimum of analysis, the roles previously played by $\xi_c = d\sigma/2 = \sigma/(2\sqrt{\lambda})$ and $\sigma_c = 2\xi/d = 2\xi\sqrt{\lambda}$ are filled instead by

$$\xi_{c,0} = \frac{d_0\sigma}{2} = \frac{\sigma}{2\sqrt{\lambda_0}} \quad \text{and} \quad \sigma_{c,0} = \frac{2\xi}{d_0} = 2\xi\sqrt{\lambda_0}. \tag{8}$$

These are the values of ξ_c and σ_c for immobile stoppers; as we shall discuss presently, they are different from ξ_c and σ_c when the stoppers have finite lifetimes. One sees from the figure that when $\xi/\xi_{c,0}$ is sufficiently small, the average velocity is almost independent of τ_s; in this "step percolation limited regime," the mean lifetime is long compared to the typical time the step takes to overgrow a stopper. The situation is, however, entirely different as $\xi/\xi_{c,0}$ approaches 1 (the regime where steps got stuck or nearly so when the stoppers were immobile). For such ξ the average velocity is affected strongly by the value of τ_s. When $\xi/\xi_{c,0} \gg 1$ the average velocity becomes almost independent of ξ; in this "stopper detachment limited regime" the step is stuck much of the time, making progress mainly when one of the stoppers that pinned it disappears. As examples, parts of two runs are provided in the Supporting Information, one done with $\tau_s = 1$, $\xi/\xi_{c,0} = 0.5$ and the other done with $\tau_s = 1$, $\xi/\xi_{c,0} = 4$ (Videos S2, S3, respectively).

To interpret this data, we observe that when the stoppers have a finite expected lifetime there is, in addition to the percolation parameter ζ defined by eqn (3), an additional nondimensional parameter

$$\mu = \frac{d}{\tau_{sc} M \sigma} = \frac{1}{\tau_{sc} M \sigma \sqrt{\lambda}} \tag{9}$$

where τ_{sc} is the mean (dimensional) stopper lifetime, λ is the (dimensional) stopper density,

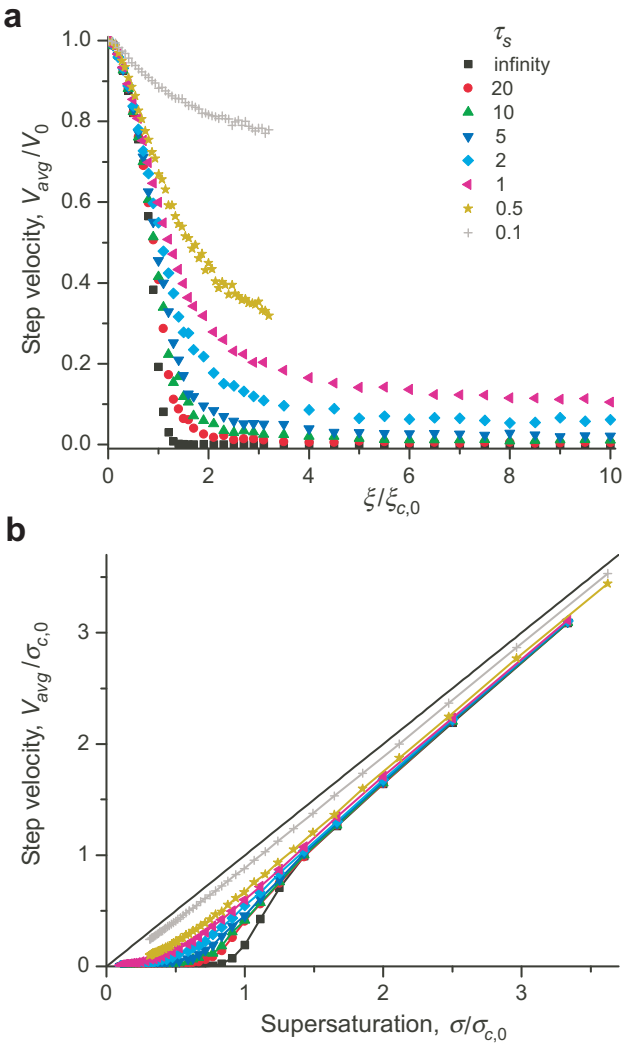

Figure 5: Average step velocity, for different values of the mean nondimensional lifetime τ_s. **(a)** $V_{\rm avg}/V_0$ as a function of $\xi/\xi_{c,0}$; **(b)** $V_{\rm avg}/\sigma_{c,0}$ as a function of $\sigma/\sigma_{c,0}$; here $\xi_{c,0}$ and $\sigma_{c,0}$ are defined by eqn (8). These simulations were done using $\lambda_0 = 20$.

and $d = 1/\sqrt{\lambda}$. Evidently, μ compares the dimensional stopper lifetime to the typical time a step moving at velocity $V_0 = M\sigma$ takes to travel the distance between stoppers. In terms of the nondimensional stopper lifetime τ_s introduced in eqn (6), μ has the alternative characterization $\mu = (d/L)/\tau_s$. By dimensional analysis, there should be a law for the average velocity of the form

$$\frac{V_{\text{avg}}}{M\sigma} = f(\zeta, \mu) \tag{10}$$

for some function f of two variables. To determine the function f from the results of our simulations, we must deal with two difficulties:

(a) the density of stoppers is not constant over the course of the simulation; and

(b) the simulations estimate the value of f only at selected points in the (ζ, μ) plane.

We deal with point (b) by interpolation, of course (after some smoothing of the data, since the numerically-determined V_{avg} is the output of a stochastic simulation, and is therefore noisy). Concerning point (a): recall that our simulation has a parameter λ_0, the expected number of stoppers in a 1×1 square. When we distribute stoppers in a 1×0.1 rectangle ahead of the front, the number of stoppers is chosen from a Poisson distribution with mean $\lambda_0/10$, assuring that the density of stoppers in the rectangle is λ_0. However if the stoppers have finite lifetimes then *the density decreases as they disappear*, by eqn (7).

To understand how our data provide information about the function $f(\zeta, \mu)$ we must account for this effect. To do so, we observe that if the average velocity is well-defined, then the times t_k at which new stoppers are laid down in the simulation are (approximately) multiples of some period τ_p. Neglecting stochasticity, the period τ_p can be determined from the average velocity. ζ and μ are periodic functions of the (nondimensional) simulation time t, with $\zeta(t) = \zeta_0 e^{-(t-t_k)/(2\tau_s)}$ and $\mu(t) = \mu_0 e^{(t-t_k)/(2\tau_s)}$ as t ranges over the period $t_k < t < \tau_p + t_k$ (The exponential function is used because stopper lifetimes are modeled

with Poisson distributions with mean lifetime τ_s). Their mean values are thus

$$\bar{\zeta} = \zeta_0 \frac{2\tau_s}{\tau_p} \left(1 - e^{-\tau_p/(2\tau_s)}\right), \tag{11}$$

$$\bar{\mu} = \mu_0 \frac{2\tau_s}{\tau_p} \left(e^{\tau_p/(2\tau_s)} - 1\right). \tag{12}$$

If the velocity of the interface is given by eqn (10) at every time t, then what we report as $V_{\rm avg}$ (the time-averaged velocity of the interface) is actually

$$V_{\rm avg} = \frac{M\sigma}{\tau_p} \int_0^{\tau_p} f(\zeta(t), \mu(t))\, dt. \tag{13}$$

Since we do not know the form of f (indeed, we are trying to find f from data about $V_{\rm avg}$), we need an approximation of eqn (13) that does not depend on the form of f. In analyzing our data, we used the approximation

$$\frac{1}{\tau_p} \int_0^{\tau_p} f(\zeta(t), \mu(t))\, dt \approx f(\bar{\zeta}, \bar{\mu}),$$

Using these approximations, each simulation done at finite τ_s determines the value of f at an associated point $(\bar{\zeta}, \bar{\mu})$ in the (ζ, μ) plane. As already noted, given such data, smoothing and interpolation permit evaluation of the function f throughout the region of the (ζ, μ) plane that was explored by our simulations.

Using this technique, we calculated the average velocity $V_{\rm avg} = M\sigma f(\zeta, \mu)$ as a function of ζ or σ, for several values of the dimensional stopper lifetime

$$\tau_{sc} = \frac{\tau_s d\sqrt{\lambda_0}}{M\sigma}.$$

This formula agrees with eqn (6) since $\lambda_0 = \lambda L^2$. The results are shown in Figure 6. The trends we observed in Figure 5 are essentially unchanged; in particular, when ζ is small the average velocity is insensitive to stopper detachment, and for $\zeta \gg 1$ the average velocity is

almost independent of ζ. Dwelling a bit on the latter regime, when the motion of the step is stopper-detachment-limited: it is natural to expect that $V_{\rm avg}/V_0$ should be proportional to $d/(\tau_{sc}V_0)$, since d/V_0 is the time it takes a step (in the absence of stoppers) to travel distance d. Such proportionality was also predicted in an earlier analysis of a similar growth regime.[51] We do not expect the constant of proportionality to be 1 since (i) the local velocity of our step is usually smaller than V_0, and (ii) the typical distance to the next stopper above a point on the step is only proportional to d, not equal to d. Our data confirms the anticipated proportionality: indeed, using simulations done with $\lambda_0 = 20$ and fixing $\zeta = 2.7$, we find that $V_{\rm avg}/V_0 \approx 0.51(2)/\tau_{sc}$ (Figure 7).

In experimental work on crystal growth, kinetic data are usually reported as $V(c)$, where c is concentration of the inhibitor in the growth medium. We expect the stopper density, λ, to be proportional to c, so ζ is proportional to $\sqrt{c}$ in this setting; see eqn (3). For a high density of weakly bound stoppers (high ζ and low τ_{sc}), our kinetic curves resemble those associated with the Bliznakov mechanism,[52,53] in which impurity molecules do not pin steps but only make attachment to kinks slower. Mathematically, for the Bliznakov mechanism one has $V = (1-\theta)V_0 + \theta V_\infty$, where θ measures the surface coverage by the impurity, V_0 is the step velocity in the absence of impurities, and V_∞ is the step velocity with full coverage by the impurities ($\theta = 1$). It is natural to model the surface coverage using the Langmuir isotherm: $\theta = Kc/(1+Kc)$, where K is the adsorption constant; then the prediction of the Blizkanov mechanism becomes

$$\frac{V}{V_0} = 1 - \left(1 - \frac{V_\infty}{V_0}\right)\theta = 1 - \alpha\frac{Kc}{1+Kc}, \tag{14}$$

where $0 < \alpha < 1$ is a system-dependent and supersaturation-dependent constant.

In the large-ζ regime the results of our simulations are very similar to those predicted by (14). Since c is proportional to ζ^2, it is natural to start by considering $V_{\rm avg}/V_0$ as a function of ζ^2 rather than ζ: Figure 8a does this, using the same data as Figure 6, for values of ζ up

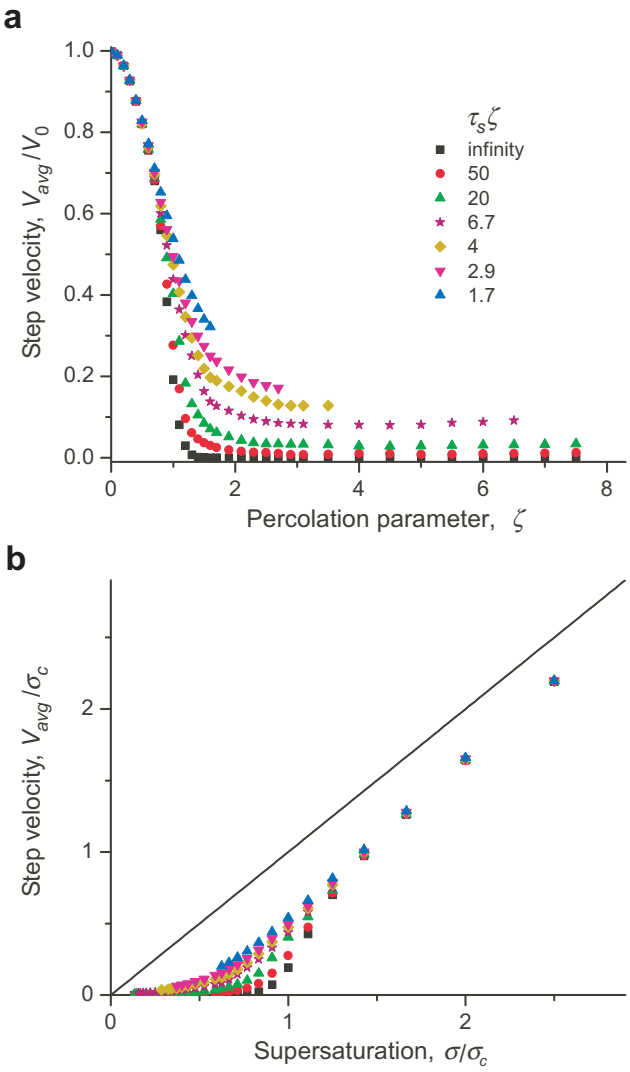

Figure 6: Average step velocity for different values of the mean nondimensional lifetime $\tau_s\zeta$. **(a)** $V_{\rm avg}/V_0$ as a function of $\zeta = \xi/\xi_c$; **(b)** $V_{\rm avg}/\sigma_c$ as a function of $\zeta^{-1} = \sigma/\sigma_c$. These simulations were done using $\lambda_0 = 20$.

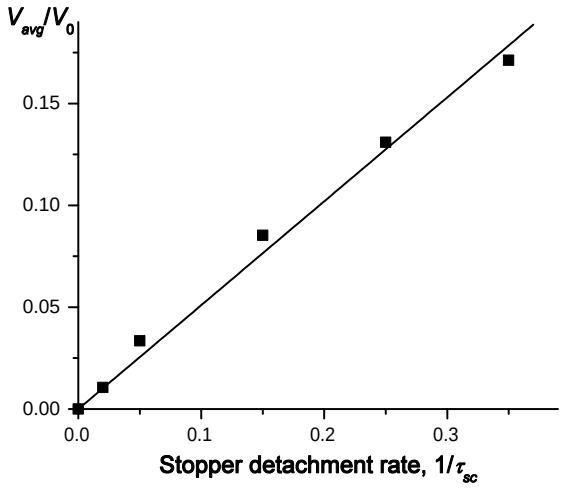

Figure 7: Average step velocity $V_{\rm avg}/V_0$ as a function of dimensional stopper detachment rate $1/\tau_{sc}$, for $\zeta = 2.7$. These simulations were done with $\lambda_0 = 20$.

to about 3. Since $V_0 = M\sigma$, eqn (14) predicts that $V(c)$ should depend roughly linearly on supersaturation, σ[2,3] (we use here that c and K are independent of supersaturation, and α is only weakly dependent on it). Our simulations are consistent with this: $V_{\rm avg}$ is nearly a linear function of σ for $\sigma/\sigma_c = 1/\zeta < 0.4$ (Figure 8b).

The similarity between Cabrera-Vemilyea and Bliznakov inhibition kinetics for a high density of weakly bound stoppers is not surprising, since these conditions substantially suppress cooperativity in the action of impurity stoppers. The possibility of considering two types of inhibition kinetics within one framework was considered before,[27] but our simulations provide a physical basis for connecting the C-V and Bliznakov mechanisms. We emphasize that the underlying physics of the C-V mechanism remains different from that of Bliznakov in the high-ζ, low-τ_{sc} regime; but the associated kinetics are similar, because in this regime the stoppers impede the propagation of the step without developing strong cooperativity. This similarity in the consequences of the two growth inhibition mechanisms means that it is difficult to distinguish between them using only kinetic data.

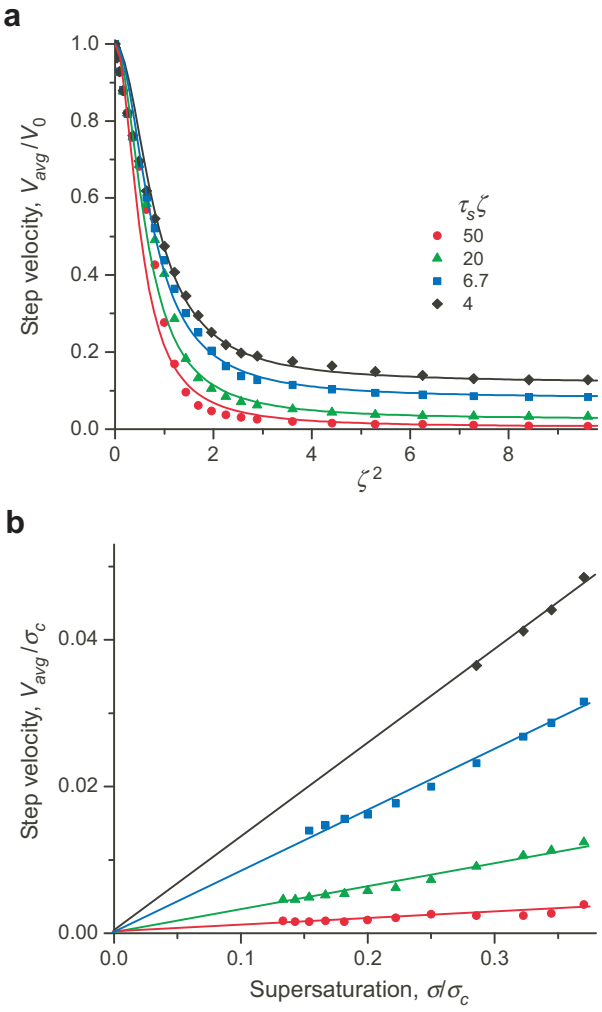

Figure 8: (**a**) $V_{\rm avg}/V_0$ as a function ζ^2, using the same data as for Figure 6 (note that the concentration is proportional to ζ^2); (**b**) $V_{\rm avg}/\sigma_c$ as a function of $\sigma/\sigma_c = 1/\zeta$, when ζ is large. Solid lines represent fitting to Bliznakov inhibition kinetics eqn (14).

Conclusions

We have studied how the macroscopic velocity of a step is affected by the presence of randomly-located stoppers with finite or infinite lifetimes. This was done using a continuum model for the evolution of the step, simulated numerically using a front-tracking-based numerical method. Our continuum model is a generalization of the one formulated by Cabrera and Vermilyea in 1958: our stoppers pin the moving interface unless/until they are overgrown (when the pinning angle reaches the breakthrough threshold) or they disappear (if they have finite lifetimes).

It has, up to now, been a challenge to understand the quantitative consequences of this model. Indeed, the consequenes of the C-V mechanism have mainly been considered up to now for a periodic array of immobile stoppers. (A notable exception is the work of Potapenko[43], which estimates the density of randomly-located immobile stoppers required to fully arrest the motion of a step.) Our starting point is the observation that this problem is well-suited to numerical simulation, since there are just two nondimensional parameters, ζ and μ, and the macroscopic velocity is determined by a function $f(\zeta, \mu)$. We have shown that f can be determined by simulations, and have used the results to discuss the consequences of our version of the Cabrera-Vermilyea inhibition model. Thus, we have refined the classic Cabrera-Vermilyea inhibition model and extended its applicability to a wider spectrum of crystal growth conditions.

When the stoppers are immobile (i.e. they never desorb) there is just one nondimensional parameter, the "percolation parameter" ζ. In this case (which corresponds to taking $\mu = 0$) we have found that shape of the kinetic curve is roughly the same for random vs periodic stoppers for low values ζ. As ζ approaches 1, however, the two cases behave very differently. In the periodic setting V_{avg} decreases sharply to 0 at a well-defined threshold $\zeta = 1$. In the random setting V_{avg} decreases much more gradually, remaining nonzero well above $\zeta = 1$. In our stochastic simulations at values of ζ up to about 1.6, some runs show the step getting stuck within the computational timeframe, but others show it continuing to make progress.

This indicates that in the context of immobile stoppers, slow crystallization should be still possible at relatively high stopper densities.

For stoppers with finite lifetimes, complete inhibition is not possible. At low ζ, the shape of the kinetic curve is almost independent of the stopper lifetime; however when ζ is large V_{avg} becomes independent of ζ, with a value that depends on the stopper lifetime.

These results improve our understanding of crystal growth inhibition mechanisms, broadening the range of systems for which we have tools to study growth inhibition quantitatively. The tools developed here should, in particular, be useful for studying systems with a high kink density where crystallization occurs at moderate supersaturation, for example ice with antifreeze proteins,[22,54] potassium dihydrogen phosphate in the presence of trivalent metals,[5] calcium oxalate monohydrate with acidic peptides,[10–13] and *L*-cystine with tailor-made additives.[19,20] The model needs further development, however, to address other common situations, especially to consider steps with low kink densities and the case of growth under a high driving force for crystallization. Growth instabilities related to slow adsorption of impurities, leading to formation of macrosteps, are another important scenario worth considering. Such instabilities have generally been modelled by considering the velocity of the step as a function of stopper density.[55–57] Our more microscopic approach offers a possible alternative, though the required simulations would be much larger than those reported here since they would need to track many steps whereas we only follow a single step. The simulation of macroscopic phenomena such as 2D pattern-formation involving macrosteps[57] would probably not be feasible using our approach, due to the large spatial and timescales on which they occur.

Supporting Information Available

The Supporting Information is available free of charge on the ACS Publications website at DOI:

Videos S1 – S3 show typical simulation runs of steps moving through arrays of stoppers. Video S1: $\zeta = 0.5$, $\tau_s = \infty$; Video S2: $\zeta = 0.5$, $\tau_s = 1$; Video S3: $\zeta = 4$, $\tau_s = 1$.

AUTHOR INFORMATION

Corresponding Authors

*(J.P.L.-T.) E-mail: leethorp@cims.nyu.edu.

*(A.G.S.) E-mail: shtukenberg@mail.ru.

*(R.V.K.) E-mail: kohn@cims.nyu.edu.

ORCID

James P. Lee-Thorp: 0000-0001-6445-7155

Alexander G. Shtukenberg: 0000-0002-5590-4758

Robert V. Kohn: 0000-0002-4386-6889

Notes

The authors declare no competing financial interest.

Acknowledgement

This work was supported primarily by the MRSEC Program of the National Science Foundation under Award Number DMR-1420073. RVK acknowledges additional support from NSF grant DMS-1311833.

References

(1) Sangwal, K. Additives and crystallization processes: from fundamentals to applications; John Wiley & Sons, 2007.

(2) De Yoreo, J. J.; Vekilov, P. G. In Biomineralization; Dove, P. M., De Yoreo, J. J., Weiner, S., Eds.; Mineralogical Society of America Geochemical Society: Washington, DC, USA, 2003; Vol. 54; pp 57–93.

(3) Shtukenberg, A. G.; Ward, M. D.; Kahr, B. Crystal growth with macromolecular additives. Chem. Rev. **2017**, 117, 14042–14090.

(4) Cabrera, N.; Vermilyea, D. A. In Growth and perfection of crystals; Doremus, R., Roberts, B., Turnbell, D., Eds.; Wiley: New York: Cooperstown, NY, 1958; pp 393–410.

(5) Rashkovich, L.; Kronsky, N. Influence of Fe^{3+} and Al^{3+} ions on the kinetics of steps on the {100} faces of KDP. J. Cryst. Growth **1997**, 182, 434–441.

(6) Shekunov, B. Y.; Grant, D. J.; Latham, R. J.; Sherwood, J. N. In situ optical interferometric studies of the growth and dissolution behavior of paracetamol (acetaminophen) crystals. 3. Influence of growth in the presence of p-acetoxyacetanilide. J. Phys. Chem. B **1997**, 101, 9107–9112.

(7) Ristić, R.; Shekunov, B. Y.; Sherwood, J. N. Growth of the tetrahedral faces of sodium chlorate crystals in the presence of dithionate impurity. J. Cryst. Growth **1994**, 139, 336–343.

(8) Weaver, M. L.; Qiu, S. R.; Hoyer, J. R.; Casey, W. H.; Nancollas, G. H.; De Yoreo, J. J. Improved model for inhibition of pathological mineralization based on citrate–calcium oxalate monohydrate interaction. ChemPhysChem **2006**, 7, 2081–2084.

(9) Weaver, M. L.; Qiu, S. R.; Hoyer, J. R.; Casey, W. H.; Nancollas, G. H.; De Yoreo, J. J. Inhibition of calcium oxalate monohydrate growth by citrate and the effect of the background electrolyte. J. Cryst. Growth **2007**, 306, 135–145.

(10) Weaver, M. L.; Qiu, S. R.; Hoyer, J. R.; Casey, W. H.; Nancollas, G. H.; De Yoreo, J. J. Surface aggregation of urinary proteins and aspartic acid-rich peptides on the faces of calcium oxalate monohydrate investigated by in situ force microscopy. Calcif. Tissue Int. **2009**, 84, 462–473.

(11) Weaver, M. L.; Qiu, S. R.; Friddle, R. W.; Casey, W. H.; De Yoreo, J. J. How the overlapping time scales for peptide binding and terrace exposure lead to nonlinear step dynamics during growth of calcium oxalate monohydrate. Cryst. Growth Des. **2010**, 10, 2954–2959.

(12) Friddle, R. W.; Weaver, M. L.; Qiu, S. R.; Wierzbicki, A.; Casey, W. H.; De Yoreo, J. J. Subnanometer atomic force microscopy of peptide–mineral interactions links clustering and competition to acceleration and catastrophe. Proc. Natl. Acad. Sci. U. S. A. **2010**, 107, 11–15.

(13) Cho, K. R.; Salter, E. A.; De Yoreo, J. J.; Wierzbicki, A.; Elhadj, S.; Huang, Y.; Qiu, S. R. Growth inhibition of calcium oxalate monohydrate crystal by linear aspartic acid enantiomers investigated by in situ atomic force microscopy. CrystEngComm **2013**, 15, 54–64.

(14) Davis, K. J.; Dove, P. M.; De Yoreo, J. J. The role of Mg^{2+} as an impurity in calcite growth. Science **2000**, 290, 1134–1137.

(15) Wasylenki, L. E.; Dove, P. M.; De Yoreo, J. J. Effects of temperature and transport conditions on calcite growth in the presence of Mg^{2+}: Implications for paleothermometry. Geochim. Cosmochim. Acta **2005**, 69, 4227–4236.

(16) Wasylenki, L. E.; Dove, P. M.; Wilson, D. S.; De Yoreo, J. J. Nanoscale effects of strontium on calcite growth: An in situ AFM study in the absence of vital effects. Geochim. Cosmochim. Acta **2005**, 69, 3017–3027.

(17) Van Driessche, A. E. S.; Sazaki, G.; Dai, G.; Otalora, F.; Gavira, J. A.; Matsui, T.; Yoshizaki, I.; Tsukamoto, K.; Nakajima, K. Direct observation of adsorption sites of protein impurities and their effects on step advancement of protein crystals. Cryst. Growth Des. **2009**, 9, 3062–3071.

(18) Sleutel, M.; Van Driessche, A. E. S. On the self-purification cascade during crystal growth from solution. Cryst. Growth Des. **2013**, 13, 688–695.

(19) Shtukenberg, A. G.; Poloni, L. N.; Zhu, Z.; An, Z.; Bhandari, M.; Song, P.; Rohl, A. L.; Kahr, B.; Ward, M. D. Dislocation-actuated growth and inhibition of hexagonal L-cystine crystallization at the molecular level. Cryst. Growth Des. **2015**, 15, 921–934.

(20) Poloni, L. N.; Zhu, Z.; Garcia-Vázquez, N.; Yu, A. C.; Connors, D. M.; Hu, L.; Sahota, A.; Ward, M. D.; Shtukenberg, A. G. Role of molecular recognition in L-cystine crystal growth inhibition. Cryst. Growth Des. **2017**, 17, 2767–2781.

(21) Sangwal, K. Kinetic effects of impurities on the growth of single crystals from solutions. J. Cryst. Growth **1999**, 203, 197–212.

(22) Vorontsov, D. A.; Sazaki, G.; Hyon, S.-H.; Matsumura, K.; Furukawa, Y. Antifreeze effect of carboxylated ε-poly-L-lysine on the growth kinetics of ice crystals. J. Phys. Chem. B **2014**, 118, 10240–10249.

(23) Miura, H.; Tsukamoto, K. Role of impurity on growth hysteresis and oscillatory growth of crystals. Cryst. Growth Des. **2013**, 13, 3588–3595.

(24) Miura, H. Numerical study of impurity-induced growth hysteresis on a growing crystal surface. Cryst. Growth Des. **2016**, 16, 2033–2039.

(25) Punin, Y. O.; Artamonova, O. I. Growth rate hysteresis of KH_2PO_4 crystals. Kristallografiya **1989**, 34, 1262–1266.

(26) Kubota, N.; Yokota, M.; Doki, N.; Guzman, L. A.; Sasaki, S.; Mullin, J. W. A mathematical model for crystal growth rate hysteresis induced by impurity. Cryst. Growth Des. **2003**, 3, 397–402.

(27) Kubota, N.; Mullin, J. W. A kinetic model for crystal growth from aqueous solution in the presence of impurity. J. Cryst. Growth **1995**, 152, 203–208.

(28) Ristic, R. I.; DeYoreo, J. J.; Chew, C. M. Does impurity-induced step-bunching invalidate key assumptions of the Cabrera-Vermilyea model? Cryst. Growth Des. **2008**, 8, 1119–1122.

(29) Land, T. A.; Martin, T. L.; Potapenko, S.; Palmore, G. T.; De Yoreo, J. J. Recovery of surfaces from impurity poisoning during crystal growth. Nature **1999**, 399, 442–445.

(30) Potapenko, S. Y. Moving of step through impurity fence. J. Cryst. Growth **1993**, 133, 147–154.

(31) van Enckevort, W. J. P.; Van den Berg, A. C. J. F. Impurity blocking of crystal growth: a Monte Carlo study. J. Cryst. Growth **1998**, 183, 441–455.

(32) Lutsko, J. F.; González-Segredo, N.; Durán-Olivencia, M. A.; Maes, D.; Van Driessche, A. E. S.; Sleutel, M. Crystal growth cessation revisited: The physical basis of step pinning. Cryst. Growth Des. **2014**, 14, 6129–6134.

(33) Ranganathan, M.; Weeks, J. D. Theory of impurity induced step pinning and recovery in crystal growth from solutions. Phys. Rev. Lett. **2013**, 110, 055503.

(34) Ranganathan, M.; Weeks, J. D. Impurity effects in crystal growth from solutions: Steady states, transients and step bunch motion. J. Cryst. Growth **2014**, 393, 35–41.

(35) van Enckevort, W. J. P.; Los, J. H. "Tailor-made" inhibitors in crystal growth: A Monte Carlo simulation study. J. Phys. Chem. C **2008**, 112, 6380–6389.

(36) Sleutel, M.; Lutsko, J. F.; Maes, D.; Van Driessche, A. E. S. Mesoscopic Impurities Expose a Nucleation-Limited Regime of Crystal Growth. Phys. Rev. Lett. **2015**, 114, 245501.

(37) De Yoreo, J. J.; Zepeda-Ruiz, L. A.; Friddle, R. W.; Qiu, S. R.; Wasylenki, L. E.; Chernov, A. A.; Gilmer, G. H.; Dove, P. M. Rethinking classical crystal growth models

through molecular scale insights: Consequences of kink-limited kinetics. Cryst. Growth Des. **2009**, 9, 5135–5144.

(38) Lutsko, J. F.; Van Driessche, A. E. S.; Durán-Olivencia, M. A.; Maes, D.; Sleutel, M. Step crowding effects dampen the stochasticity of crystal growth kinetics. Phys. Rev. Lett. **2016**, 116, 015501.

(39) Sleutel, M.; Lutsko, J. F.; Van Driessche, A. E. S. Mineral growth beyond the limits of impurity poisoning. Cryst. Growth Des. **2018**, 18, 171–178.

(40) Kupier, M.; Morton, C.; Abraham, S.; Gray-Weale, A. The biological function of an insect antifreeze protein simulated by molecular dynamics. eLife **2015**, 4, e05142.

(41) Lee-Thorp, J. P.; Shtukenberg, A. G.; Kohn, R. V. Effect of step anisotropy on crystal growth inhibition by immobile impurity stoppers. Cryst. Growth Des. **2017**, 17, 5474–5487.

(42) Miura, H. Phase-field modeling of step dynamics on growing crystal surface: step pinning induced by impurities. Cryst. Growth Des. **2015**, 15, 4142–4148.

(43) Potapenko, S. Y. Threshold for step percolation through impurity fence. J. Cryst. Growth **1993**, 133, 141–146.

(44) Armstrong, S.; Cardaliaguet, P. Stochastic homogenization of quasilinear Hamilton–Jacobi equations and geometric motions. J. Eur. Math. Soc. **2018**, 20, 797–864.

(45) Caffarelli, L. A.; Monneau, R. Counter-example in three dimension and homogenization of geometric motions in two dimension. Arch. Rational Mech. Anal. **2014**, 212, 503–574.

(46) Dirr, N.; Yip, N. K. Pinning and de-pinning phenomena in front propagation in heterogeneous media. Interfaces Free Bound. **2006**, 8, 79–109.

(47) Coville, J.; Dirr, N.; Luckhaus, S. Non-existence of positive stationary solutions for a class of semi-linear PDEs with random coefficients. Netw. Heterog. Media **2010**, 5, 745.

(48) Dirr, N.; Dondl, P. W.; Scheutzow, M. Pinning of interfaces in random media. Interfaces Free Bound. **2011**, 13, 411–421.

(49) Bodineau, T.; Teixeira, A. Interface motion in random media. Comm. Math. Phys. **2015**, 334, 843–865.

(50) Dondl, P. W.; Scheutzow, M. Ballistic and sub-ballistic motion of interfaces in a field of random obstacles. Ann. Appl. Probab. **2017**, 27, 3189–3200.

(51) Voronkov, V. V.; Rashkovich, L. N. Step kinetics in the presence of mobile adsorbed impurity. J. Cryst. Growth **1994**, 144, 107–115.

(52) Bliznakov, G. Sur le méchanisme de l'action des additifs adsorbants dans la croissance cristalline. Adsorption et croissance cristalline. Editions du Centre Nat. de la Recherche Sci. **1965**, 291–301.

(53) Chernov, A. A. Modern crystallography III: Crystal growth; Springer, 1984; Vol. 36.

(54) Kubota, N. Effects of cooling rate, annealing time and biological antifreeze concentration on thermal hysteresis reading. Cryobiology **2011**, 63, 198–209.

(55) van der Eerden, J. P.; Müller-Krumbhaar, H. Dynamic coarsening of crystal surfaces by formation of macrosteps. Phys. Rev. Lett. **1986**, 57, 2431–2433.

(56) van der Eerden, J. P.; Müller-Krumbhaar, H. Formation of macrosteps due to time dependent impurity adsorption. Electrochim. Acta **1986**, 31, 1007–1012.

(57) Kandel, D.; Weeks, J. D. Kinetics of surface steps in the presence of impurities: Patterns and instabilities. Phys. Rev. B **1995**, 52, 2154–2164.

For Table of Contents Use Only

Crystal growth inhibition by mobile randomly distributed stoppers

James P. Lee-Thorp, Alexander G. Shtukenberg, and Robert V. Kohn

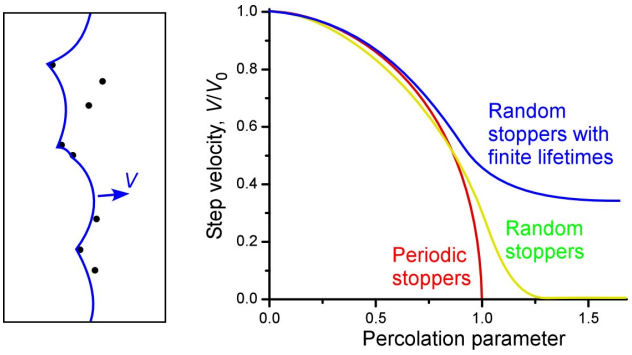

Synopsis: To refine the classical Cabrera-Vermilyea step pinning model, a semi-implicit front tracking algorithm was used to simulate growth inhibition by randomly distributed stoppers with finite lifetimes. It was shown that compared to periodic placement, a random distribution of stoppers results in a much more gradual decrease of the average step velocity to its asymptotic value, zero in the case of permanent stoppers and some non-zero value for stoppers with finite lifetimes.